Super-Resolution Fluorescence Microscopy Reveals Nanoscale Catalytic Heterogeneity on Single Copper Nanowires

Matthew Jun Kit Ow[#], Jia Jun Ng[#], Jian Xiong Yong[#], Benjamin Yi Liang Quek, Edwin K. L. Yeow, and Zhengyang Zhang*

Division of Chemistry and Biological Chemistry, School of Physical and Mathematical Sciences, Nanyang Technological University, 21 Nanyang Link, Singapore 637371.

[#]These authors contributed equally to this work.

*Correspondence to: zhang.zy@ntu.edu.sg

Supporting Information

Materials and Methods

Optical setup. SRM was achieved on an Olympus IX71 inverted fluorescence microscope. A circularly polarized 638-nm laser (Cobolt) was introduced to the back focal plane of an oil-immersion objective lens (Olympus UplanFl 100×, NA 1.45) via a dichroic mirror (Di02-R635-25x36, Semrock). A translation stage was used to shift the laser beams towards the edge of the objective lens such that the excitation light reached the sample at incidence angles close to the critical angle of the coverglass-water interface to achieve total internal reflection (TIR) wide-field illumination. Emission was filtered by a long-pass (BLP01-635R-25, Semrock) filter, and focused by an achromatic lens (f = 75 mm) onto a sCMOS camera (ORCA-Flash4.0 V2, Hamamatsu Photonics). The sample was mounted and imaged on the setup with 638-nm excitation.

Bulk fluorescence analysis. Bulk fluorescence analysis was performed on a Varian Cary Eclipse fluorescence spectrophotometer equipped with a xenon pulse lamp and a high-performance photomultiplier detector. Scan speed of 1 scan per minute was selected and the excitation wavelength was set to be 640 nm and each scan measured from 645 nm to 750 nm. 50mM of (4-{[bis-(1-tert-butyl-1H-[1,2,3]triazol-4-ylmethyl)-amino]-methyl}-[1,2,3]triazol-1-yl)-acetic acid (BTTAA), 10mg/mL of copper nanowire, 100mM of freshly prepared sodium ascorbate (NaAsc), 60 μM – 85 μM of azide fluorophore and 85 μM – 100 μM of phenylacetylene stock solutions were prepared and used for the determination of kinetics based on the variation of copper nanowires concentration, azide fluorophore concentration and phenylacetylene concentration.

Reaction rate dependence on azide concentration. For the determination of kinetics based on variation of azide fluorophore concentration, 3.2 μL of 10 mg/ml copper nanowire, 2 μL of 50 mM BTTAA, 50 μL of fresh 100 mM sodium ascorbate, 1 μL – 75 μL of 85 μM azide, 859.8 - 933.8 μL of ultrapure water were prepared in eppendorf tubes. The solution was measured using fluorescence at initial state before 10 μL of 100 mM phenylacetylene was added. Final concentrations consist of 100 μM BTTAA, 500 μM copper nanowire, 5 mM sodium ascorbate, and 1 mM phenylacetylene, with azide concentrations of 0.085 μM, 0.255 μM, 0.425 μM, 0.595 μM, 0.85 μM, 1.275 μM, 1.7 μM, 2.125 μM, 2975 μM, 3825 μM, 5100 μM and 6375 μM. Each reaction was scanned 10 times. Another variation for the determination of kinetics based on variation of azide fluorophore concentration was conducted using 60 μM of azide fluorophore. 3.2 μL of 10 mg/ml copper nanowire, 2 μL of 50 mM BTTAA, 50 μL of fresh 100 mM sodium ascorbate, 90 – 165 μL of 60 μM azide and 769.8 - 844.8 μL of ultrapure water were prepared in eppendorf tubes. The solution was measured using fluorescence at initial state before 10 μL of 100 mM phenylacetylene was added. Final concentrations consist of 100 μM BTTAA, 500μM copper nanowire, 5 mM sodium ascorbate, and 1 mM phenylacetylene, with azide concentrations of 5.4 μM, 6.3 μM, 7.5 μM, 8.7 μM and 9.9 μM. Each reaction was scanned 10 times.

Reaction rate dependence on alkyne concentration. For the determination of kinetics based on the variation of alkyne concentration, 3.2 µL of 10 mg/ml copper nanowire, 2 µL of 50 mM BTTAA, 50 µL of fresh 100 mM sodium ascorbate, 10 µL of 85 µM azide and 434.8 - 934.3 µL of ultrapure water were prepared in eppendorf tubes. The solution was measured using fluorescence at initial state before 0.5 µL – 500 µL of 100 mM phenylacetylene was added. For higher concentration measurements, 100 – 300 µL of 1M phenylacetylene was used instead. Final concentrations consist of 100 µM BTTAA, 500 µM copper nanowire, 5 mM sodium ascorbate, and 850 nM azide, with phenylacetylene concentrations of 0.05 mM. 0.1 mM, 0.3 mM, 0.5 mM, 1 mM, 5 mM, 10 mM, 20 mM, 30 mM, 50 mM, 100 mM, 200 mM and 300 mM. Each reaction was scanned 10 times. Another variation for the determination of kinetics based on variation of alkyne concentration was conducted using 85 µM of phenylacetylene. 3.2 µL of 10mg/ml copper nanowire, 2 µL of 50 mM BTTAA, 50 µL of fresh 100 mM sodium ascorbate, 10 µL of 85 µM azide and 859.8 - 933.8 µL of ultrapure water were prepared in eppendorf tubes. The solution was measured using fluorescence at initial state before 1 µL – 75 µL of 85 µM phenylacetylene was added. Final concentrations consist of 100 µM BTTAA, 500 µM copper nanowire, 5 mM sodium ascorbate, and 0.85 µM azide, with phenylacetylene concentrations of 0.085 µM, 0.255 µM, 0.425 µM, 0.595 µM, 0.85 µM, 1.275 µM, 1.7 µM, 2.125 µM, 2.975 µM, 3.825 µM, 5.1 µM, 6.375 µM. Each reaction was scanned 10 times.

Reaction rate dependence on copper nanowire concentration. For the determination of kinetics based on variation of copper nanowire concentration, 0.23 µL – 32 µL of 10 mg/ml copper nanowire, 2 µL of 50 mM BTTAA, 50 µL of fresh 100 mM sodium ascorbate, 80 µL of 60 µM azide and 801 - 831.4 µL of ultrapure water were prepared in eppendorf tubes. The solution was measured using fluorescence at initial state before 35 µL of 60 µM phenylacetylene was added. Final concentrations consist of 100 µM BTTAA, 5 mM sodium ascorbate, 4.8 µM azide and 2.975 µM phenylacetylene, with copper nanowire concentrations of 35.9 µM, 42.2 µM, 50.0 µM, 62.5 µM, 82.8 µM, 125 µM, 250 µM, 1000 µM, 2000 µM, 3000 µM, 4000 µM and 5000 µM. Each reaction was scanned 10 times.

Functionalization of coverslip. Glass coverslips (Bioptechs, 40mm circular) were cleaned with piranha solution for 30 minutes before washing thoroughly with ultrapure water, dried with nitrogen and baked at 120°C for 30 minutes. The clean and dried coverslips were then agitated on an orbit shaker (Biosan PSU-10i) in a solution (4% in toluene) of 3-aminopropyltriethoxysilane (APTES) for 90 minutes. The functionalized coverslips were washed in succession with toluene, acetone, ethanol, and ultrapure water. The coverslips were stored in Milli-Q water until use.

Single molecule analysis. Single molecule imaging was carried out on the optical setup described above. 50µL of 5mg/mL copper nanowires in ethanol was drop-casted onto a functionalised glass coverslip and left to dry. The coverslip was gently rinsed with ultrapure water to remove any unbound copper nanowires and dried with nitrogen. The drop-casted coverslip was then mounted onto a flow cell (Bioptechs FCS2) using a 0.5 mm silicone gasket as spacer. Reaction solutions of azide concentration 4.25 - 170 nM were prepared by adding 500 µL of 100 mM sodium ascorbate, 20 µL of 5 0 mM BTTAA, 10 µL of 100 mM phenylacetylene, and 0.5 – 20 µL of 85µM azide, to 9450-9469.5 µL of ultrapure water. The solutions were thoroughly mixed and flowed into the cell at 1 mL/hr using a 15 mL falcon tube microfluidic sample reservoir (Elveflow) connected to a syringe pump to generate pressure and push the solution into the cell. The cell was thoroughly flushed with each solution prior to imaging. Final concentrations consist of 5 mM sodium ascorbate, 100 µM BTTAA, 100 µM phenylacetylene, and azide concentrations of 0.85 nM, 2.55 nM, 4.25 nM, 6.375 nM, 8.5 nM, 25.5 nM, 51 nM, 93.5 nM, 170 nM. The sample was illuminated with the 638-nm laser at a power of ~2 mW. The stochastic formation of individual CalFluor 647 triazole product molecules led to transient bursts of single-molecule fluorescence in the wide-field due to the dynamic reaction/dissociation of individual CalFluor 647 triazole molecules. The background signal was low due to the TIR illumination. The sCMOS camera recorded the single-molecule images at 30 frames per second for a frame size of 256×256 pixels, and typically recorded 18,000 frames for each image.

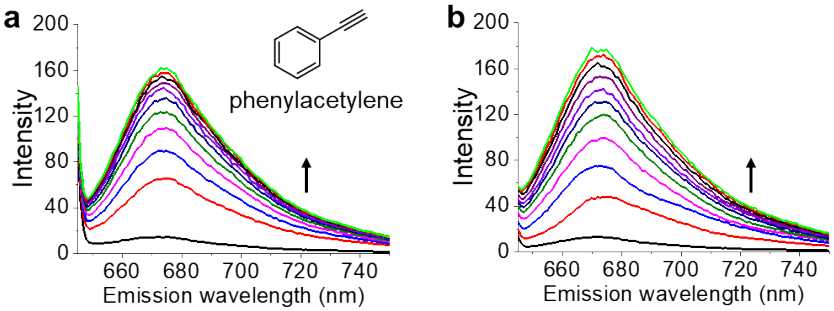

Figure S1. Ensemble fluorescence measurements of copper-nanowires-catalyzed click reaction. (a) In situ fluorescence spectra of copper-nanowires-catalyzed click reaction using 1.7 μM CalFluor 647 azide, 1 mM phenylacetylene, 100 μM BTTAA, 500 μM copper nanowires, and 5 mM sodium ascorbate. Spectra were taken at 1 min time intervals. (b) As in (a), but with 50 μM $CuSO_4$ instead of copper nanowires.

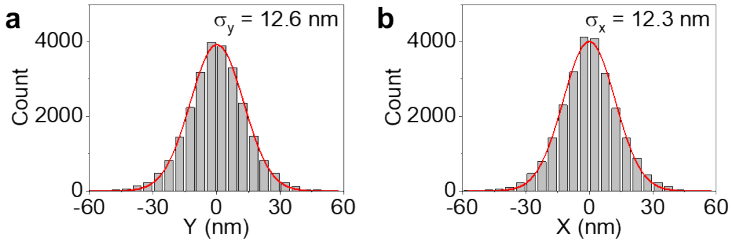

Figure S2. 2D localization distribution for CalFluor 647 triazole molecules. Clusters of localizations, either due to multiple product molecules formed at the same active site or the repetitive activation of the same product molecule, were aligned by their center of mass to generate the 2D presentation of the localization distribution. Localizations from >100 clusters (each containing >9 localizations) are summarized for CalFluor 647 triazole. Histograms of distribution in (a) *x*, (b) *y* are fitted to Gaussian functions (red curves), and the resultant standard deviations (σ_X, σ_Y) are shown in each plot.

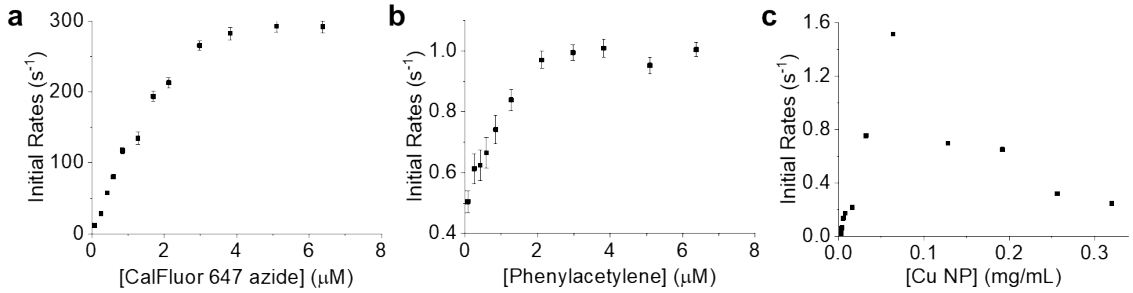

Figure S3. Ensemble catalytic kinetics of copper-nanowires-catalyzed click reaction of CalFluor 647 azide with phenylacetylene. (a) CalFluor 647 azide concentration titration of the initial reaction rate at phenylacetylene concentration of 1 mM and copper nanowires concentration of 500 μM. (b) Phenylacetylene concentration titration of the initial reaction rate at CalFluor 647 azide concentration of 0.85 μM, copper nanowires concentration of 500 μM. (c) Dependence of the initial reaction rate on the concentration of copper nanowires for click reaction using 4.8 μM CalFluor 647 azide, 2.975 μM alkyne. Initial reaction rate is defined as the production rate of the reaction product CalFluor 647 triazole.

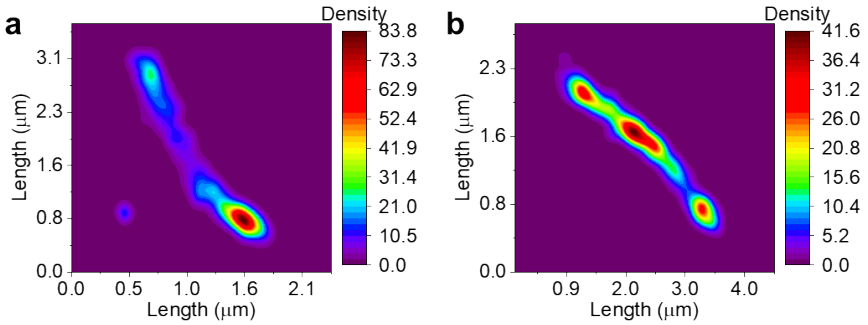

Figure S4. Two-dimensional kernel density plot of copper nanowires. (a) Plot of 2.1 μm-long copper nanowire showing higher activity at the two ends. As the ends of the copper nanowires generally have more corner and edge sites, it gives rise to higher catalytic activity than their side facets (b) Plot of 4.0 μm-long copper nanowire showing high activities at the two ends, as well as an activity gradient along the nanowire. The activity gradient is attributed to its underlying surface defect density gradient due to the direction of growth and linear decay in growth rate during synthesis.

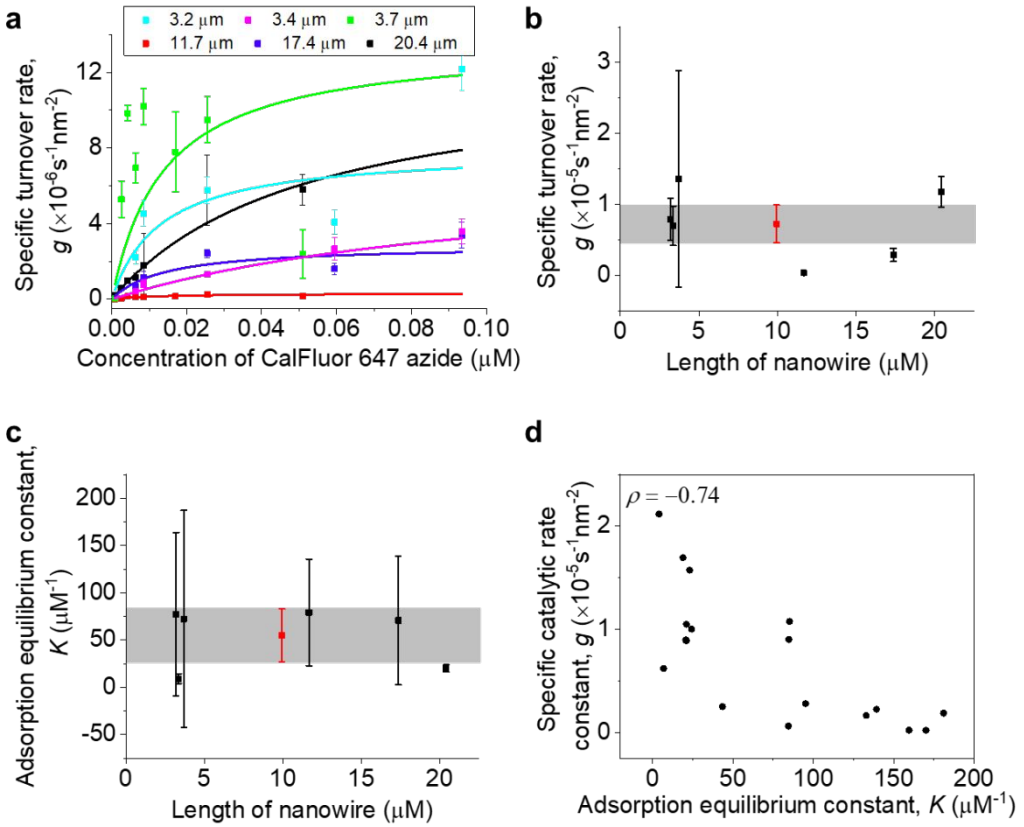

Figure S5. Reactivity rate and constants for copper nanowires of different lengths. (a) Concentration of CalFluor 647 azide dependence of specific turnover rates for single nanowires of different lengths. (b) Statistics of the specific catalytic rate constant *g* for each nanowire of different length from (a) (black) and for specific catalytic rate constant for all nanowire lengths (red). Grey band corresponds to the distribution of all nanowire lengths. (c) As in (b), but for reactant adsorption equilibrium constant *K*. (d) Correlation between specific catalytic rate constants *g* and adsorption equilibrium constant *K* of individual copper nanowires. Each data point is from a one segment of the copper nanowires. The *g* and *K* of the nanowires are anticorrelated, therefore increased catalytic activity is associated with weakened reactant adsorption.

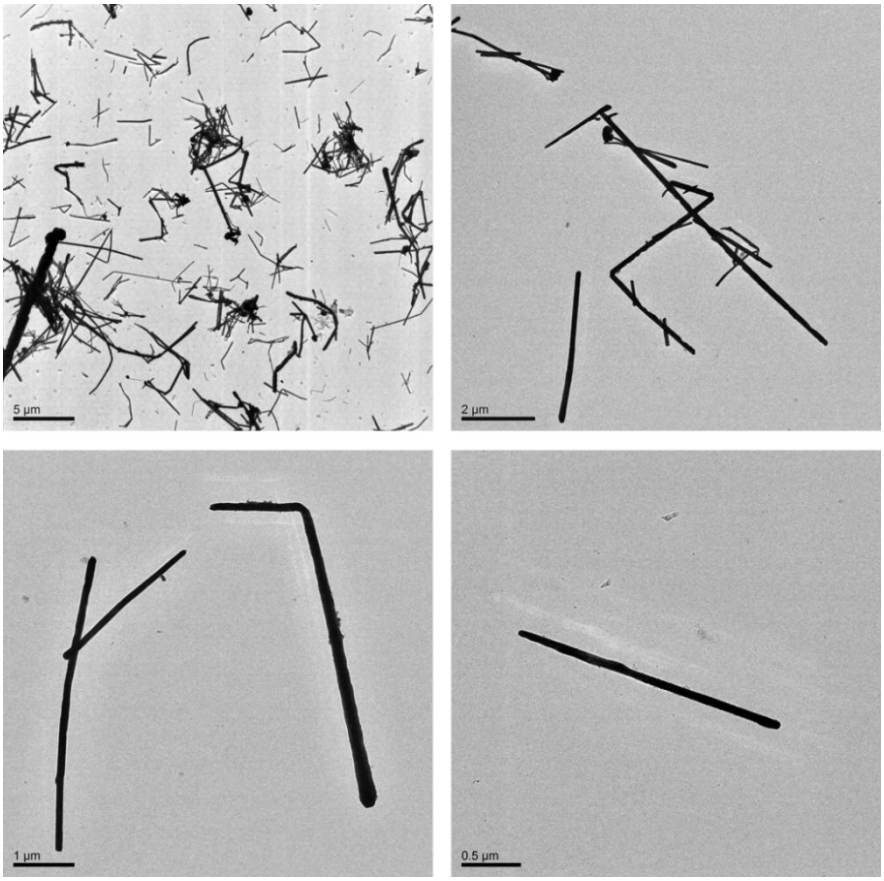

Figure S6. TEM images of copper nanowires.

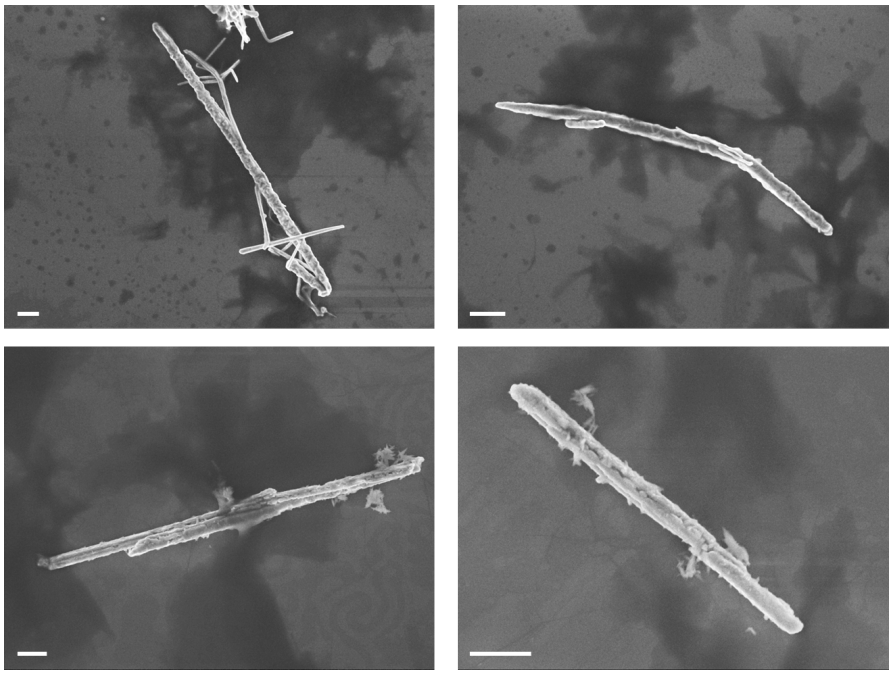

Figure S7. SEM images of copper nanowires. Scale bars: 1 µm.

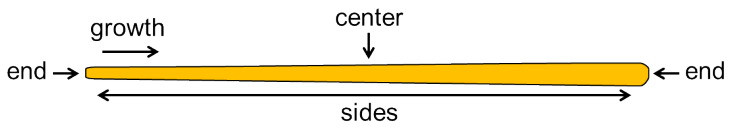

Figure S8. Schematic diagram illustrates different parts of a tapered nanowire.

Captions to Supplementary Movie

Movie S1. Part of the concurrently acquired images of single CalFluor 647 triazole molecules obtained in a catalytic reaction on a nanowire (same sample as Figure 2b). The sCMOS camera recorded at 30 frames per second (FPS), and so the playback is slowed down by 4.4-fold when played at the standard video frame rate of 25 FPS. See timestamp at the upper-left corner. Scale bar: 2 μm.